Biomechanical behaviors of dragonfly wing: relationship between configuration and deformation*

Ren Huai-Hui(任淮辉), Wang Xi-Shu(王习术)†,
Chen Ying-Long(陈应龙), and Li Xu-Dong(李旭东)

Department of Engineering Mechanics, AML, Tsinghua University, Beijing 100084, *China*

(Received 13 September 2011; revised manuscript received 8 November 2011)

In this paper, the natural structures of a dragonfly wing, including the corrugation of the chordwise cross-section, the sandwich microstructure veins, and the junctions between the vein and the membrane, have been investigated with experimental observations, and the morphological parameters of these structural features are measured. The experimental result indicates that the corrugated angle among the longitudinal veins ranges from 80° to 150°, and the sandwiched microstructure vein mainly consists of chitin and protein layers. Meanwhile, different finite element models, which include models I and I* for the planar forewings, models II and II* for the corrugated forewings, and a submodel with solid veins and membranes, are created to investigate the effects of these structural features on the natural frequency/modal, the dynamical behaviors of the flapping flight, and the deformation mechanism of the forewings. The numerical results indicate that the corrugated forewing has a more reasonable natural frequency/modal, and the first order up-down flapping frequency of the corrugated wing is closer to the experimental result (about 27.00 Hz), which is significantly larger than that of the planar forewing (10.94 Hz). For the dynamical responses, the corrugated forewing has a larger torsional angle than the planar forewing, but a lower flapping angle. In addition, the sandwich microstructure veins can induce larger amplitudes of torsion deformation, because of the decreasing stiffness of the whole forewing. For the submodel of the forewing, the average stress of the chitin layer is much larger than that of the protein layer in the longitudinal veins. These simulative methods assist us to explain the flapping flight mechanism of the dragonfly and to design a micro aerial vehicle by automatically adjusting the corrugated behavior of the wing.

Keywords: aerodynamics, corrugation, warping deformation, finite element analysis

PACS: 45.50.–j, 46.70.Hg, 87.10.Kn, 87.15.La **DOI:** 10.1088/1674-1056/21/3/034501

1. Introduction

Scientists have proposed many mathematical and mechanical models to explain the flapping flight of insects, and have performed many experiments. It has been verified that dragonfly wings can generate large lift forces and thrust, which makes dragonflies fly faster and more flexibly than other insects. When a dragonfly beats its four wings harmoniously, coupled bending and torsional deformations along the chordwise and the spanwise directions occur respectively. Ellington deduced that the dragonfly was unable to use the clap and fling mechanism, and had to rely on isolated rotation of the wings.[1] The flight behavior of the dragonfly is accompanied with a flexion of the wing to obtain additional aerodynamic forces. Therefore, the complex motions cause the wing to rotate along its trailing edge, which produces a leading edge vortex of the correct sense for the subsequent translation.[2,3] If most of the opposite vortexes have already been shed as the following flapping commences, the wing will achieve a net circulation of the correct sense. It is called the flex mechanism, and has not been validated yet. Therefore, the complex flight mechanism of the dragonfly has led to many disputes.

Previous investigations mainly focus on the aerodynamic behavior, and a rigid wing model was used to study the interaction between the structure and the atmosphere. Flexible wings with corrugation are rarely considered. For example, Hertel compared the arrangement of the longitudinal veins in dragonfly wings to the cross-sections of man-made girders.[3,4] Rees confirmed that the corrugated structural feature greatly increased both the stiffness and the strength

*Projects supported by the National Natural Science Foundation of China (Grant Nos. 10772091 and 11072124), the National Basic Research Program of China (Grants No. 2010CB631006), and the State Key Laboratory of Advanced Metals and Materials, China (Grant No. 2010ZD-03).

†Corresponding author. E-mail: xshuwang@tsinghua.edu.cn

© 2012 Chinese Physical Society and IOP Publishing Ltd

of insect wings.[5] Rees and Newman *et al.* further demonstrated that a corrugated wing was a good aerofoil at low Reynolds numbers.[6,7] Newman and Wootton have shown that the corrugation itself might have a structural role, further stiffening the wing by means of the stressed skin effect. They also discussed modes of failure and suggested that the corrugated structure allowed the wing to deform without damage when the wings suffered from large impact loadings.[7,8] Ennos have suggested the importance of torsion in the design of insect wings. He thought insect wings could be described as corrugated membranes that incorporated stiffening vein branches serially from a V-section leading edge spar.[9] Kim *et al.* reported the effects of the wing corrugation on the aerodynamic performance.[4,10] In summary, those authors mainly considered the macroscopical structural features of the dragonfly or the other insects and discussed their corrugated behaviors in two dimensions. With the development of experimental technology, the microstructures of wing veins and membrane have been discovered recently, whether the microstructure features affect the deformation and the flight behavior of the dragonfly wings has drawn much attention.[11,12]

In this paper, we investigate the structural features of wing corrugation and the microstructures of the veins and the membrane with the help of different experimental devices. Then natural frequency/modal and the dynamic responses of the total wing during the flapping process are studied by using the finite element method (FEM). In order to investigate the effects of these structural features on the dynamic behavior of the dragonfly wings, four different FE models of the forewings are created. Compared with the planar wings, more accurate corrugated forewings in three dimensions are taken into account subsequently. The veins with sandwich microstructure features are implanted into the dragonfly forewings, the detailed kinematical analysis of the different models are conducted and discussed.

2. Experimental methods

The dragonflies used in this work were Pantala flavesens, which were collected on the campus of Tsinghua University. In order to obtain the most authentic experimental data, all dragonfly samples were alive before testing, and the tests were performed within 10 min.

The dragonfly forewings were cut into several pieces along the longitudinal veins without any special treatment. The cross-section configuration of the forewing was observed by using a digital optical microscope (HC Inc., XHC-SVI DOM). Spanwise cross-sections were collected to observe the planar configuration (Fig. 1(a)) and the depth of corrugation (Fig. 1(b)), which was about 5–8 mm and gradually decreased from the root to the extent along the chordwise and the spanwise.[13,14] The patterns of the magnified wing cross-sections were photographed to study the local topological structure of the corrugation.[14–16]

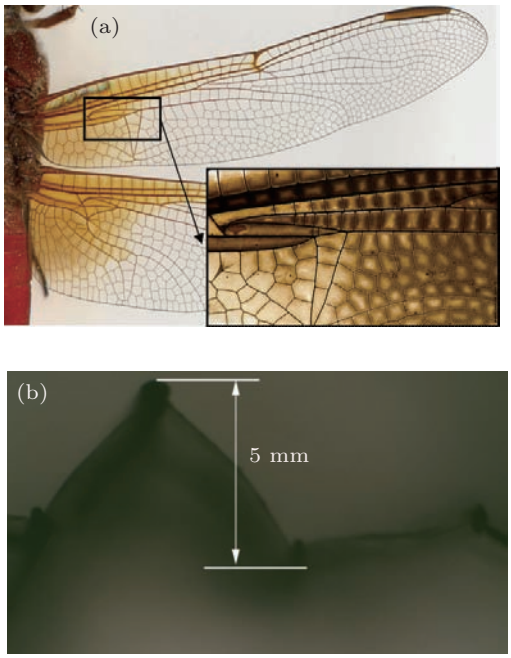
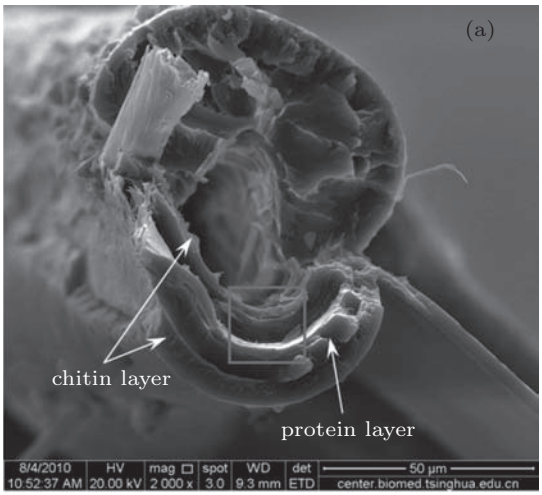


Fig. 1. (colour online) Images of wings: (a) patterns of overall wings, (b) corrugated configuration in the chordwise cross-section.

In addition, the microstructures of the veins and the membranes were observed by using environmental scanning electron microscopy (FEI Inc., Quanta 200 ESEM-FEG). Before being placed into the high vacuum environment, the cross-sections of the veins were treated by liquid nitrogen for 2–3 min. With the help of the ESEM-FEG technology, the meso and the nano structures of the wing veins were further investigated. The cross-sections of the longitudinal veins were characterized by the sandwich tubular-shaped structure with chitin and protein layers containing some fibrils,[11,17] which were different from the tubular elements reported in other research (Fig. 2).



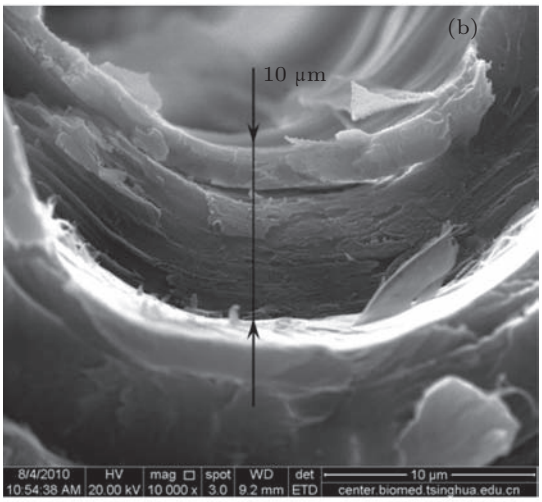


Fig. 2. Sandwich microstructure of the wing vein. (a) Cross-section of longitudinal vein. (b) Local magnified cross-section of the chitin and protein layers.

3. Mechanical model of deformation

In the biomechanical model of the dragonfly wing, the zigzag chordwise cross-section and the tubular-shaped longitudinal veins with the sandwich microstructure, which contain two dissimilar elastic media (chitin and protein), are modeled as shown in Fig. 3. Rees compared the mechanical properties of four different models, and calculated the load-bearing capacities of those structures as beams or spars in his works.[5,6] However, the effects of the alterable tubular diameter and membrane thickness along the wing on the flight performances were not considered in his models.

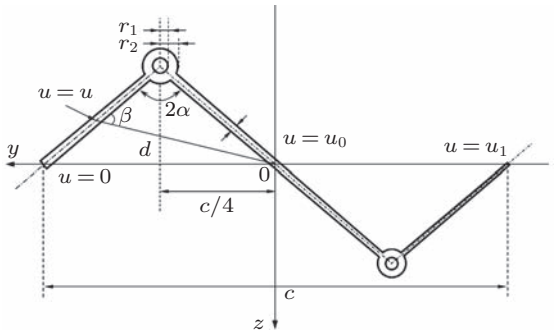


Fig. 3. Corrugated cross-section sketch of the mechanical model along the chordwise

When the dragonfly beats its wings, the torque M_{T} representing the wing deformation includes two components[18]

$$M_{\mathrm{T}} = GJ\partial^2\theta/\partial x^2 - E\Gamma\partial^4\theta/\partial x^4, \tag{1}$$

where θ is the torsional angle of deformation. The first term is the moment described by Saint–Venant's theory of torsion, and the second term is the warping moment. Torsional constant J and warping constant Γ for a thin wing ($c/t > 10$) are given by[15]

$$J = 1/3\int_0^{u_1} t^3(u)\,\mathrm{d}u + J_x(r_{\mathrm{m}}, r_{\mathrm{n}}), \tag{2}$$

$$\Gamma = \int_0^{u_1}\left(\int_{u_0}^{u} d\sin\beta\,\mathrm{d}u\right)^2 t(u)\,\mathrm{d}u + (1/12) \times \int_0^{u_1}(\mathrm{d}\cos\beta)^2 t^3(u)\,\mathrm{d}u + \Gamma_x(r_{\mathrm{m}}, r_{\mathrm{n}}), \tag{3}$$

where u is the displacement along the wing's cross-section, d is the distance between u and u_0, c is the chordwise length, and β is the angle between the line tangential to the wing section at u and the line connecting u and u_0. For the real structure of the dragonfly wing (Fig. 1(a)), the corrugation of the wing has an irregular configuration, it forms serial zigzag cross-sections by changing the different pitch values of the longitudinal veins or the leading edge spars (Fig. 1(b)). The warping of the wing's cross-section is not equal to zero at $u = u_0$. The other geometrical parameters, such as thickness t of the membrane, tubular outer radius r_{m}, and inner radius r_{n}, can be defined to have functions of u. Their values gradually decrease along the wings' spanwise and chordwise directions.[11,12]

4. FE modeling of dragonfly wing

4.1. Natural structural characteristics of forewings

Although there are some structural differences between the forewing and the hindwing of a drag-

onfly, their mechanism of torsional deformation in flight can be viewed as the same. The natural structural system and the biomechanical behaviors of the forewing are completely investigated in our series of studies. A dragonfly wing consists mainly of a network of veins and membranes besides the nodus and the pterostigma. The span length of the dragonfly forewing is about 44 mm, and its average chord width is about 10–12 mm. The diameter of the major longitudinal veins ranges from 0.03 mm to 0.15 mm, the average value is about 0.07 mm, and the thickness of the membrane varies from 0.005 mm to 0.01 mm. The veins and the membranes attenuate from the root to the edge along the spanwise and the chordwise, respectively. According to these general structural features, the planar forewing model I is created at first (Fig. 4(a)). The veins in this model are defined to have a beam-like tubular-shaped structure (TSS), and consist completely of chitin.

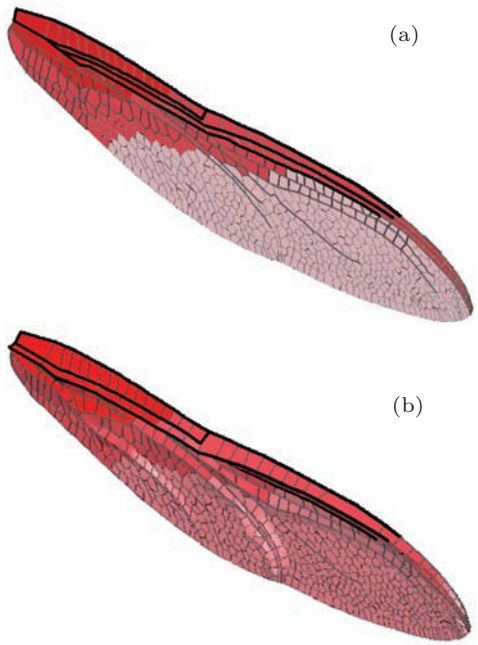


Fig. 4. (colour online) FE models of forewing: (a) planar forewing model I, (b) corrugated forewing model II.

In addition, other important structural features, such as the corrugation of the cross-section and the microstructure of the veins, are also characterized. Then corrugated forewing model II is created (Fig. 4(b)), and the same veins of TSS are implanted into it. Although the planar patterns of the corrugated forewing are very similar to that of the planar forewing, there is a significant difference at the wing's cross-section, especially the camber configuration.[19,20] The corrugation is one of the most crucial characteristics of the wing (Fig. 5(a)). In general, the zigzag cross-section can cause some alterable geometrical channels on the wing's surface and vary with the distance along the spanwise from large to small, which can produce rather larger trailing edge vortexes. Therefore, vortexes are produced not only by the airfoil shape of the dragonfly wing but also by the alterable channels causing the corrugated behavior. The membrane colors from fuscous to weak red and the vein colors from black to grey in the forewing models stand for different thicknesses of the membranes and different diameters of the veins, respectively (Fig. 5(b)).

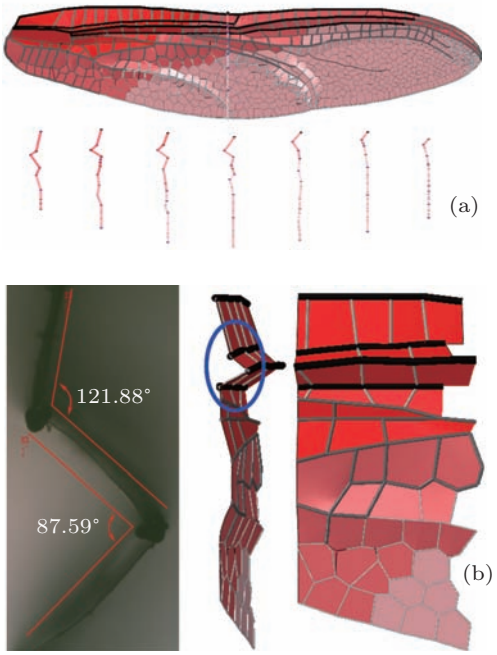


Fig. 5. (colour online) Characteristics of the corrugated forewing. (a) Different chordwise cross-sections along the spanwise direction of the forewings. (b) Comparison of the experimental image and the typical corrugated configuration in the FE modeling.

With respect to the microstructural features of the veins, they are no longer regarded as the simple tubular-shaped beams reported by previous studies.[8,9] The characteristics of the longitudinal veins with more detailed structures are accurately defined in accordance with the experimental observations. Therefore, the beam elements integrated by using a meshed cross-section modeling approach are implanted into the wing system. The beam profile of the longitudinal vein is firstly meshed with two-dimensional warping elements, then it is integrated numerically into the model to obtain the beam stiffness and the beam inertia properties. Two different beam cross-sections are integrated to characterize the longitudinal veins in the forewing, so two new forewing models are derived subsequently. They are the planar wing model I*, whose veins are defined as the open sandwich structure (OSS) shown in Fig. 6(a),

and the corrugated wing model II*, whose veins are defined as the open sandwich structure with an angle about 120° (OSSA) shown in Fig. 6(b). The relationships among the torsional, the bending, and the warping deformations with different beam profiles are calculated, and the numerical integration of the meshed beam can also provide the stiffness and the inertia statistics: integrated axial stiffness $\sum_i E_i A_i$, integrated bending stiffness $(\sum_i E_i I_i)_{\alpha\beta}$, integrated shear stiffness $(\sum_i G_i A_i)_{\alpha\beta}$, total mass per unit length $\sum_i \rho_i A_i$, and rotary inertia $(\sum_i \rho_i I_i)_{\alpha\beta}$. With regard to the tubular-shaped structure (TSS), all physical parameters of the TSS, the OSS, and the OSSA models are listed in Table 1. We can find that the parameters of the TSS model, such as mass, axial and shear stiffnesses, are larger than those of the the other two models, and the OSS and the OSSA models have approximately the same axial and shear stiffnesses. The differences of these parameters mainly result from the different microstructural features and the material properties of the veins. Two dissimilar elastic materials appear in the longitudinal veins,[11,21] including the chitins of isotropic elastic material (Young's modulus $E = 1650$ MPa, Poisson's ratio $\upsilon = 0.25$) and the protein of elastic material ($E = 1.6$ MPa, $\upsilon = 0.45$). For the isotropic elastic membrane, the parameters are very different in some papers,[12,16] so averaged values are used in this study ($E = 400$ MPa, $\upsilon = 0.30$).

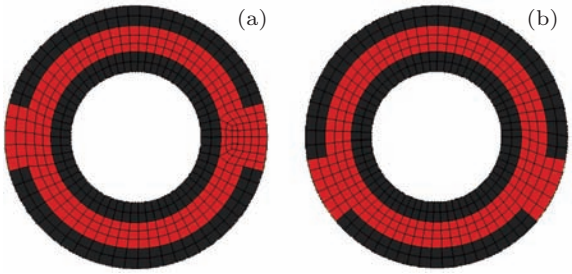


Fig. 6. (colour online) (a) OSS model and (b) OSSA model of the vein cross-section.

When the geometrical models of the planar and the corrugated forewings are created, the forewings are meshed by different element types. The membranes are meshed by linear quadrilateral shell elements of type S4 and triangular shell elements of type S3 respectively, and the veins are meshed by linear beam elements of type B31. There are 19086 nodes and 25820 elements in the corrugated forewing, while 18156 nodes and 24753 elements in the planar forewing.

Table 1. Mechanical parameters of TSS, OSS, and OSSA models.

Typical model	Mass /10^{-5}mg·mm^{-1}	EA /MPa·mm^2	EI_{11} /MPa·mm^4	EI_{12} /MPa·mm^4	EI_{22} /MPa·mm^4	GJ /MPa·mm^2
TSS	4.24	235.53	0.18395	-9.581×10^{-7}	0.18394	0.14149
OSS	3.488	158.25	0.13274	1.043×10^{-6}	0.10642	0.07303
OSSA	3.488	158.26	0.12724	2.920×10^{-8}	0.11154	0.07312

4.2. Dynamical simulation of a flapping forewing

In order to improve the efficiency of dynamic process analysis, the modal dynamic analysis of the dragonfly wings can be carried out by using modal superposition procedures, which are different from direct-solution dynamic analysis. The natural frequency/modal of a dragonfly wing structural system needs to be extracted firstly, then the dynamic responses of the flapping forewings are resolved subsequently.

The accuracy of the numerical analysis is also affected by many physical factors, including the boundary conditions and the loading types. Most researchers directly apply a vertical uniform pressure on the dragonfly wings to simplify the interaction between the wing and the air, which can avoid complex fluid–structure interaction problems drastically.[13,22] In our studies, the applied loading is a distributed pressure along the spanwise direction (Fig. 7(a)). This kind of loading not only is similar to the real flow field, but also prevents incorrect deformation and stress singularities at the root of the wings. The weight of the dragonfly (about 380 mg) is assumed to be equal to the lift force when the dragonfly hovers in the air. So the average pressure on the surface of each wing is about 2.25×10^{-6} N/mm^2. In order to simulate the complete dynamical process of the flapping forewing, we should still define a more accurate applied loading. The vertical lift force coefficient in the ground reference describes a similar trend of the amplitude of the applied loading varying with time (Fig. 7(b)), which has been measured by many researchers.[11,13] Therefore, the distributed loading is actually a function of time and space, and it is always perpendicular to the surface of the forewing.

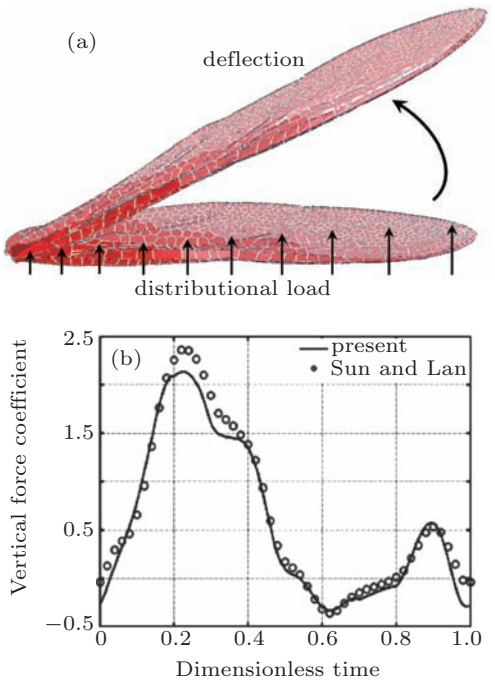


Fig. 7. (colour online) Applied loading types in the FE modeling. (a) Applied loading coupled with the corrugated forewing. (b) Vertical force coefficient changed with time.[23]

4.3. Submodel of longitudinal veins and membranes

Another technology, called submodeling, is used to reveal the detailed torsion deformation of the complex solid structure of the forewing during the process of flapping. Submodeling is a technique used in the local part of a model to refine the mesh, such as that in the junction between the vein and the membrane, based on the interpolation of solution from an initial and global model onto appropriate parts of the submodel boundary. This method is particularly effective when it is necessary to obtain an accurate and detailed solution in the local region, whereas the FE modeling of that region has a negligible influence on the overall solution. The mechanical response at the boundary of the local region is defined by solving the global model. According to the images of the experimental observation using ESEM-FEG, we design the local part of the forewing model as a submodel, which lies on the anterior of the corrugated forewing with three mainly longitudinal sandwich microstructure veins, six chordwise veins, and eight separated membranes (Fig. 8(a)). The shell-to-solid submodeling in the location of the overall forewings is created. The submodel is finely meshed by three-dimensional solid tetrahedron elements (C3D4), and the driven nodes on the solid elements are extracted to couple with the displacement and the rotation of the forewing during the flapping process (Fig. 8(b)).

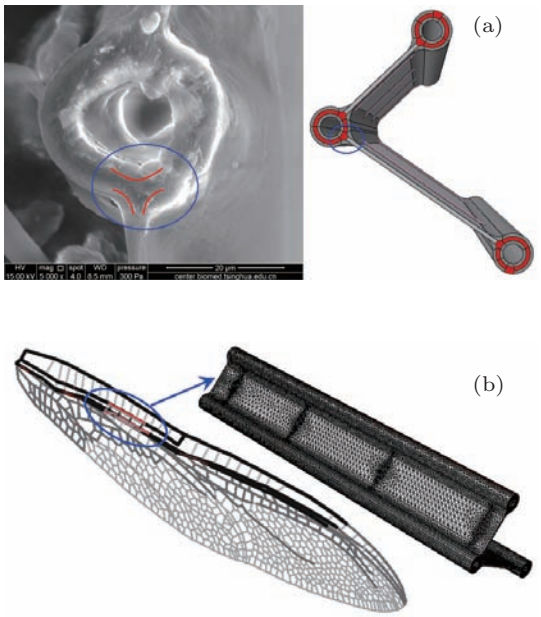


Fig. 8. (colour online) Shell-to-solid submodeling of forewings. (a) Comparison of the experimental image and part of the corrugated cross-section of the submodel. (b) Location of the submodel in the corrugated forewing.

5. Results and discussion

5.1. Natural frequencies/modals of different models

Comparing the results of natural frequency/modal extracted from the different models, as shown in Table 2, we find that the modals from the first order to the fourth order play the most significant roles in the structural deformation of the dragonfly forewings. These modals are able to reflect the mode shape of the forewing vibration, and can be named as modals of up–down flapping, bending and twisting, front–back flapping, and twisting and bending, respectively. The first order up–down flapping frequencies for the forewing models in the same dimensions are very close to each other. The first order frequencies of the planar forewings with the TSS and the OSS veins are 10.396 Hz and 9.8356 Hz, respectively. Those of the corrugated forewings with the TSS and the OSSA veins are 28.552 Hz and 28.633 Hz, respectively, which are very close to the experimental result of about 27 Hz in the vibration test.[24,25] For the planar forewings, each corresponding frequency of model I is larger than that of model I* except the fourth order frequency of twisting and bending. It is different in the corrugated forewings, the first order frequency of model II is almost the same as that of model II*, the other frequencies become lower because of the effects of the open sandwich microstructure veins on the stiffness of the forewings.

Table 1. First four order frequencies of different forewing models.

Typical model	First order frequency/Hz	Second order frequency/Hz	Third order frequency/Hz	Fourth order frequency/Hz
Model I	10.936	59.011	75.939	71.024
Model I*	9.8356	40.619	55.833	80.789
Model II	28.552	55.346	84.876	127.77
Model II*	28.633	41.900	72.038	99.149

The mode shapes of vibration for the models in the same dimensions are almost coincidental, but the amplitudes are different for the different models. The forewing models with the sandwich veins have larger amplitudes of vibration. In addition, the mode shapes of vibration for the planar and the corrugated forewings are very different, which mainly affects the torsion deformation of the forewing (Fig. 9).

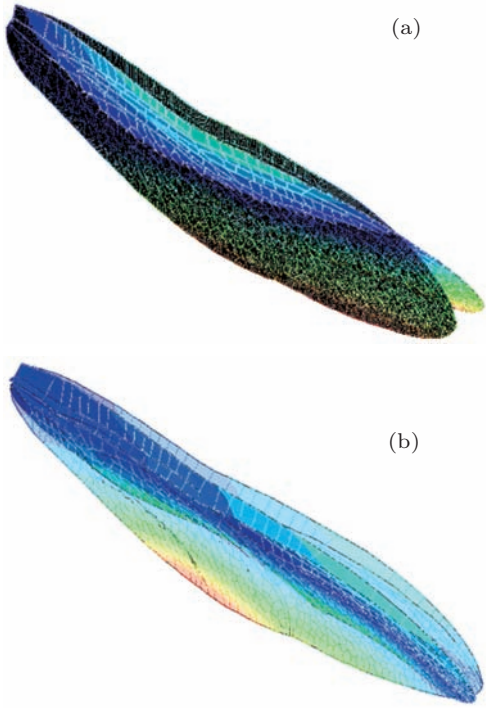


Fig. 9. (colour online) Modal of twisting and bending of forewings in models (a) I and (b) II.

It is shown that the modal of model I has a warping deformation besides the torsion, and the position of the torsion axis is ambiguous (Fig. 9(a)). However, for model II, the torsion axis of forewing lying on the subcostal, and the torsion deformations are more acceptable (Fig. 9(b)). So we can infer that the deformation of the corrugated forewing is much closer to the real one when the dragonfly beats its wings to keep hovering in the air.

5.2. Effects of natural structure on torsion deformation

The analysis of the transient dynamical responses of the forewing is carried out based on the frequency/modal extraction. The deformations and the von Mises stress distributions of the forewing for models I and II are presented in Figs. 10(a) and 10(b), respectively. Obviously, there are different dynamical responses under the same applied loading. The major deformation of the planar forewing is bending along the body of the dragonfly. The corrugated forewing has a larger torsion angle than that of the planar forewing, but a lower flapping angle. The reasons (Fig. 10(b)) include many factors. One of the most important factors is the effects of the zigzag cross-sections of the longitudinal veins on the corrugated behavior of the forewing, which are obviously different from that of the planar forewing. For the corrugated forewing with OSSA veins, the torsion particularly dominates the deformation behavior of the dragonfly forewing, so the torsion angle of model II* (Fig. 10(d)) is larger than that of model II (Fig. 10(c)) when the maximum spatial displacement is achieved. The result of the dynamical analysis indicates that the torsion deformation arises from a structural response during the flapping process of the forewing, which depends strongly on the natural structure of the corrugated cross-section, the sandwich microstructure veins, and the organic junction between the veins and the membranes. From the viewpoint of energy, for the corrugated forewings, the energy needed to produce the bending deformation is less than that for the planar forewings when resisting the same external loading. It means that more energy is used to produce the warping and the torsion deformations for the corrugated wings. The larger torsion deformation of the corrugated forewing makes it easy to produce the lift force required in flight. Meanwhile, there is

a salient difference between the von Mises stress distributions for the two models (Figs. 10(a) and 10(b)). The maximum stress in the planar forewing appears in the larger geometrical regions. But the stress in the corrugated forewing is more favorable to the strength of the wing. In addition, it is very conducive to preventing the wings from damaging the thin and brittle membrane under high stress levels.

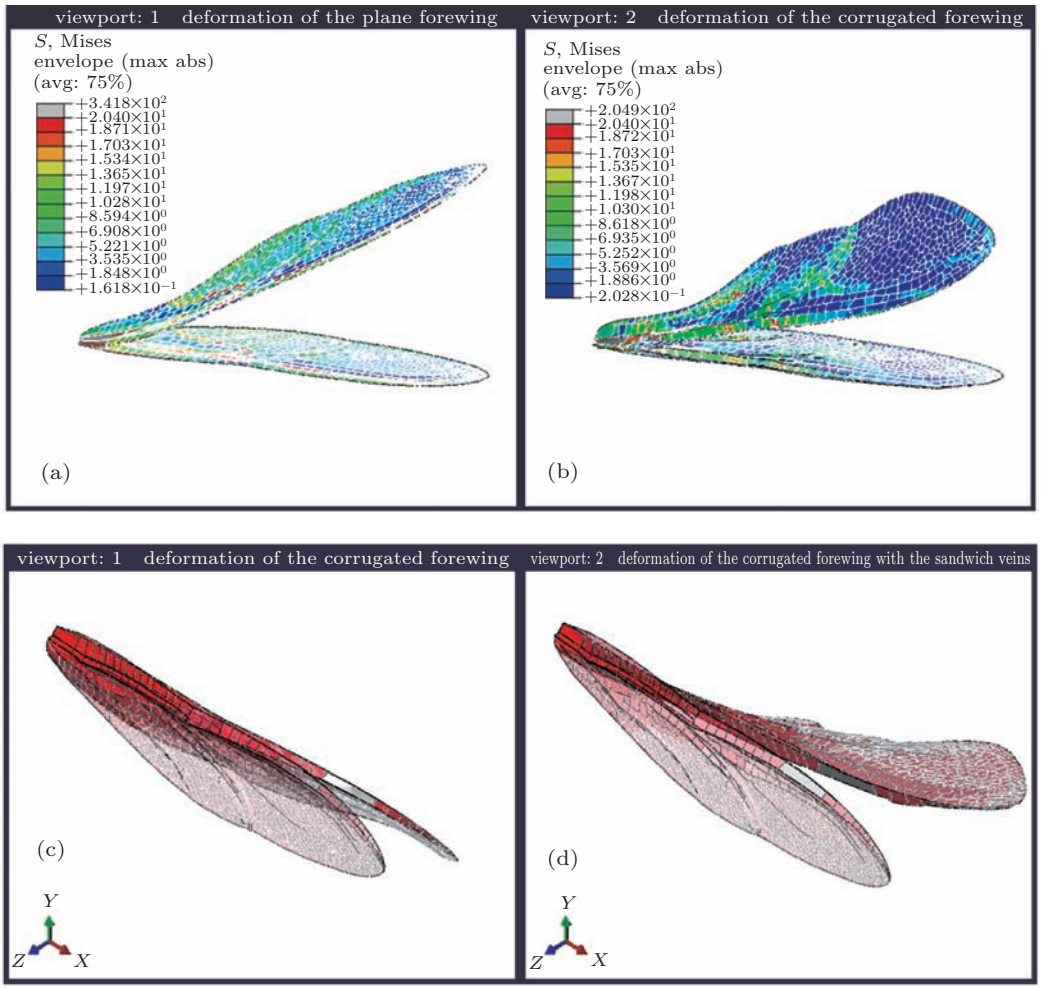


Fig. 10. (colour online) Deformations and stress distributions of the forewings in models (a) I, (b) II, (c) II, and (d) II*.

5.3. Numerical analysis of the wing submodel

The submodel of the corrugated forewing is created according to the boundary conditions driven by the displacement of the global model. The deformation and the von Mises stress contours of the submodel regions under the greatest applied loading are shown in Fig. 11. Because of the deformation of the global model, the 3-dimensional solid submodel shows an obviously spatial displacement (Fig. 11(a)) relative to the initial position. Meanwhile, the submodel produces a significant structural deformation, the corrugated angle of radius between the adjacent membranes increases gradually along the spanwise direction. Many inaccurate stresses and deformations appear on the edge of the submodel, which are caused by the imprecise boundary displacements from the global model. However, the stress and the deformation away from the bonder of the submodel can be also thought to be reasonable. The zigzag cross-section in the submodel is extracted to assess the stress state of the corrugated forewing (Fig. 11(b)). It is shown that there is a significantly stress gradient between the chitin layers and the protein layer, and the maximum stress in the chitin layers is larger than that in the protein layer for the longitudinal veins. Therefore, the chitin layers always bear a higher applied load to prevent the protein

layer from damage in flight.

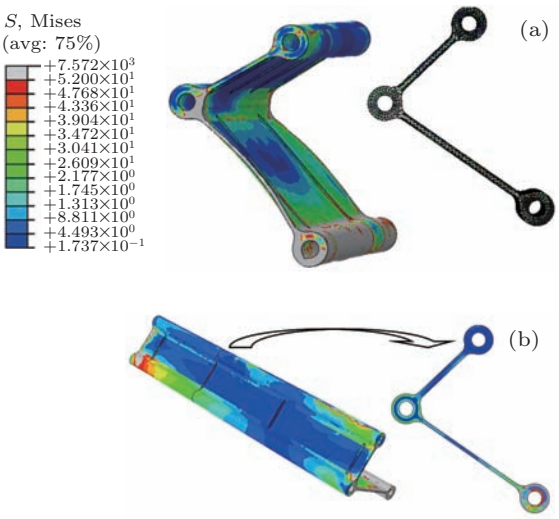


Fig. 11. (colour online) Von Mises stress contours in a 3-dimensional solid structural submodel. (a) Deformation and stress relative to the initial position in submodel. (b) Von Mises stress contours in the submodel cross-section.

6. Conclusion

With the help of a digital optical microscope and an environmental scanning electron microscope, the structural features of a dragonfly wing including the corrugation of the chordwise cross-section, the sandwich microstructure veins, and the organic junction between the veins and the membranes are investigated. The experimental results indicate that the corrugated angle among the longitudinal veins range from 80° to 150°, and the sandwich microstructure veins mainly consist of chitin layers and protein layers. It means that the zigzag cross-section configuration of the wing can easily cause relative movement among the longitudinal veins, so the camber with the channels can produce more vortexes to increase the lift force of the dragonfly. Meanwhile, the different FE models, models I and I* for the planar forewings, models II and II* for the corrugated forewings, and the submodel with solid veins and membranes, are created to investigate the effects of these structural features on the natural frequencies/modals, the dynamical behaviors of the flapping flight, and the deformation mechanism of the forewings. By comparing with the simulation results of the structural models, some major conclusions are drawn as follows.

1) Based on the meshed beam cross-section modeling technique, the mechanical parameters of the veins, which are defined as the TSS, the OSS, and the OSSA models, are calculated. The results indicate that the axial and the shear stiffnesses of the veins with the sandwich microstructure are much lower than that of the traditional tubular-shaped veins, which makes the whole wing more flexible.

2) Compared to the planar forewings, the corrugated forewings are more reasonable in natural frequency and modal, especially for the modal of twisting and bending, which mainly affects the torsion deformation of the wing. The first order frequencies of the corrugated forewings with the TSS (model II) and the OSSA (model II*) model veins are 28.552 Hz and 28.633 Hz, respectively, which are very close to the experimental result of about 27 Hz.

3) By comparing the dynamical responses of different models, the effects of the structural features, including the corrugation of the cross-section and the sandwich microstructure of the veins, on the dynamical behaviors of the dragonfly forewing are investigated. The results indicate that the corrugated forewing has a larger torsional angle than the planar forewing, but a lower flapping angle. The complex structural deformation of the corrugated wings (model II) mainly ascribes to the zigzag cross-section of the longitudinal veins. In addition, the sandwich microstructure veins induce larger amplitudes of torsion deformation in response to the decreased stiffness of the whole forewing. It means that the effect of the structural features, especially the microstructure of the vein, on the flight performance of wing cannot be ignored.

4) A three-dimensional solid structural submodel is created to investigate the detailed deformation and the stress distributions of the forewing with the sandwich microstructure veins and the membranes. The von Mises stress and the warping deformation on the corrugated cross-section of the forewing can be estimated quantitatively. The maximum stress in the chitin layers is larger than that in the protein layer in the longitudinal veins. These simulative methods can help to explain the flapping flight mechanism of the wing very well and to design a micro aerial vehicle by automatically adjusting the corrugated behavior of the wing.

References

[1] Ellington C P 1984 *Philoso. T. R. Soc.* B **305** 41

[2] Azuma A 1985 *J. Exp. Biol.* **116** 79

[3] Hertel H 1966 *Structure, Form, Movement* (New York: Reinhold)

[4] Zhao G Z, Yu X J and Xu Y 2010 *Chin. Phys.* B **19** 070203

[5] Rees C J C 1975 *Nature* **256** 200

[6] Fu J L, Zhao W J and Weng Y Q 2008 *Chin. Phys.* B **17** 2361

[7] Newman J S and Wootton R J 1986 *J. Exp. Biol.* **125** 361

[8] Wootton R J, Evans K E, Herbert R and Smith C W 2000 *J. Exp. Biol.* **203** 2921

[9] Ennos A R 1988 *J. Exp. Biol.* **140** 137

[10] Kim W K, Ko J H, Park H C and Byun D Y 2009 *J. Theor. Biol.* **260** 523

[11] Wang X S, Li Y and Shi Y F 2008 *Compos. Sci. Technol.* **68** 186

[12] Song F, Xiao K W, Bai K and Bai Y L 2007 *Mat. Sci. Eng.* **457** 254

[13] Ennos A R and Wootton R J 1989 *J. Exp. Biol.* **143** 267

[14] Okamoto M, Yasuda K and Azuma A 1996 *J. Exp. Biol.* **199** 281

[15] Sunada S, Zeng L J and Kawachi K 1998 *J. Theor. Biol.* **193** 39

[16] Li Z X, Shen W, Tong G S, Tian J M and Loc V Q 2009 *J. Zhejiang Univ. Sci.* A **10** 72

[17] Zhao H X, Yin Y J and Zhong Z 2010 *Chin. Sci. Bull.* **55** 1993

[18] Chen Y L, Wang X S, Ren H H and Li X D 2011 *Chin. Sci. Bull.* **56** 1658

[19] Sun M and Tang J 2002 *J. Exp. Biol.* **205** 55

[20] Luo G Y and Sun M 2005 *Acta Mech. Sin.* **21** 531

[21] Sun J Y, Pan C X, Tong J and Zhang J 2010 *IET Nanobiotechnol.* **4** 10

[22] Lehmann F O 2006 *Arthropod Struct. Dev.* **209** 5005

[23] Wang Y T, Kalyanasundaram S and Young J 2008 *Australasian Conference on Robotics and Automation* (*ACRA 2008*) (Australia: Australian Robotics and Automation Association) p. 6

[24] Chen J S, Chen J Y and Chou Y F 2008 *J. Sound Vib.* **313** 643

[25] Beliveau J G, Vigneron F R, Soucy Y and Draisey S 1986 *J. Sound Vib.* **107** 435